

## Enhanced Co orbital moments in Co-rare-earth permanent-magnet films

D. J. Keavney, Eric E. Fullerton, Dongqi Li, C. H. Sowers, and S. D. Bader  
Argonne National Laboratory, Materials Science Division, Argonne, Illinois 60439

K. Goodman and J. G. Tobin

Department of Chemistry and Materials Science, Lawrence Livermore National Laboratory, Livermore, California 94550

R. Carr

Stanford Linear Accelerator Center, Stanford Synchrotron Radiation Laboratory, Stanford, California 94309

(Received 17 March 1997; revised manuscript received 30 June 1997)

Soft x-ray magnetic circular dichroism (MCD) data were collected at the Co  $L$  edges from a series of epitaxial  $R$ -Co ( $R$ =Pr, Nd, Sm, Dy, and Ho) intermetallic compound films grown by sputter deposition. The Co orbital-to-spin moment ratios were extracted from the data using the MCD sum rules. An enhanced Co orbital moment, as compared to that of bulk hcp-Co, is seen in all but one of the films. The enhancement is dependent on both the average  $R$ -Co bond length and on the  $R$  species. These results suggest that a significant transition-metal (TM) orbital moment is the origin of the TM sublattice contribution to the magnetocrystalline anisotropy energy in  $R$ -TM compounds. [S0163-1829(98)05409-5]

### I. INTRODUCTION

The highest performance permanent magnet materials are currently rare-earth-transition-metal ( $R$ -TM) intermetallics and borides,<sup>1,2</sup> for example  $\text{SmCo}_5$  and  $\text{Nd}_2\text{Fe}_{14}\text{B}$ . In these materials, a predominantly  $R$  spin-orbit interaction yields the high magnetocrystalline anisotropy (MCA) required for a high coercivity. The TM, usually Fe or Co, is coupled to the  $R$  and enhances the saturation magnetization ( $M_s$ ), and therefore the theoretical maximum energy product,  $(4\pi M_s)^2/4$ . Although the large orbital moment of the  $R$   $4f$  shell dominates the anisotropy energy especially at low temperatures, there is evidence that the anisotropy energy contribution from the TM is enhanced above its bulk value. Specifically, permanent magnet compounds in which the  $R$  that has no  $4f$  orbital moment can also have high MCA. For example, the Y-Co system forms compounds that are isostructural with several well-known  $R$ -Co permanent magnets, such as  $\text{SmCo}_5$  and  $\text{Sm}_2\text{Co}_{17}$ . Some of these compounds have anisotropy fields ( $H_A$ ) two orders of magnitude higher than that of bulk Co, and  $H_A$  does not have a monotonic dependence on the  $R$  content<sup>3-6</sup> Similar anisotropy fields are observed for the lanthanides with  $L=0$ .<sup>7</sup> Such high anisotropies suggest that the Co atoms possess a significant orbital moment coupled to the lattice, with a corresponding increase in the anisotropy energy. The existence of large orbital moments in such compounds has not been directly observed, however, mainly because orbital moment data are difficult to obtain. A large orbital moment at the Co  $2c$  site has been inferred in  $\text{YCo}_5$  from an analysis of magnetic form factors in polarized neutron scattering,<sup>8</sup> but other experimental techniques disagree on the size of the orbital moment, and on its site assignment.<sup>9</sup> The origin of any orbital moment enhancement also remains an open question. The structural dependence of the anisotropy noted above suggests that the local Co atomic environment plays a role. In this picture, a volume expansion or a reduction of available states for Co  $3d$  electrons to hybridize with could narrow the Co  $3d$  bands. This

would lead to an enhanced orbital moment closer to that of atomic Co, even though the Co  $3d$  electrons remain predominantly itinerant. It is a general feature of  $R$ -TM intermetallics that the lattice parameters contract with the  $R$  atomic size across the lanthanide series. Therefore we might expect that for the light RE's a large orbital moment is induced on the Co sites, which reduces with the lanthanide contraction.

Since its first observance, x-ray magnetic circular dichroism (MCD) (Ref. 10) has emerged as a promising technique for obtaining element specific magnetic information, especially from magnetic thin films.<sup>11-14</sup> This type of information is particularly advantageous in systems where both components are magnetic and are not separable by magnetometry,<sup>14</sup> such as in RE-TM compounds. In addition, through the use of sum rules derived in the atomic approximation, it has been found that the orbital<sup>15</sup> and spin<sup>16</sup> contributions to the total moment can be extracted from MCD spectra at the TM  $L$  edges and RE  $M$  edges. For the TM  $L$  edges the sum rules are

$$\begin{aligned} \mu_o &= - \frac{4 \int_{L_{2,3}} (I^+ - I^-) dE}{3 \int_{L_{2,3}} (I^+ + I^-) dE} n_h, \\ \mu_s &\left( 1 + \frac{7\langle T_z \rangle}{2\langle S_z \rangle} \right) \\ &= - \frac{6 \int_{L_3} (I^+ - I^-) dE - 4 \int_{L_{2,3}} (I^+ - I^-) dE}{\int_{L_{2,3}} (I^+ + I^-) dE} n_h, \end{aligned} \quad (1)$$

where  $\mu_o$  and  $\mu_s$  are the orbital and spin moments,  $I^{+(-)}$  is the absorption with the x-ray helicity parallel (antiparallel) to

TABLE I. Summary of structural and MCD data for the  $R$ -Co films.

Rare earth	$R$ at %	$a$ (Å)	$\mu_{\text{orb}}/\mu_{\text{spin}}$
hcp-Co	0.0	2.51	0.12
Pr	12.2	4.933	0.25
Pr	18.4	5.025	0.079
Nd	13.4	4.958	0.23
Nd	18.7	5.036	0.26
Sm	12.3	4.900	0.28
Sm	25.1	5.070	0.43
Dy	21.7	4.965	0.23
Dy	25.4	5.021	0.30
Ho	14.8	4.884	0.27

the magnetization,  $n_h$  is the number of  $3d$  band holes per atom, and  $\langle T_z \rangle$  is the expectation value of the magnetic dipole operator. The labels on the integrals indicate whether the integration is over the  $L_3$  edge only or over both edges. Interestingly, these sum rules appear to work well even for itinerant ferromagnets such as Fe and Co metal.<sup>17</sup> This suggests that MCD (while not a site-specific technique, as for example Mössbauer spectroscopy) may be able to shed some light on the existence of enhanced TM orbital moments and their role in the anisotropy of  $R$ -TM permanent magnets. Presently, most MCD measurements on  $R$ -TM compounds have been at the  $R$   $L$  edge or the TM  $K$  edge,<sup>18,19</sup> with relatively few soft x-ray measurements at the magnetically important TM  $L$  edge.<sup>20</sup> In this article, we apply the sum rules to Co  $L$ -edge MCD data collected from a series of epitaxial  $R$ -Co ( $R$ =Pr, Nd, Sm, Dy, and Ho) films to investigate the Co orbital moment and the role of the local Co environment in the orbital quenching.

## II. EXPERIMENT

The series of Co- $R$  films was grown by sputter deposition onto MgO(100) wafers coated with epitaxial 200 Å  $W(100)$  buffer layers. The compounds were formed by cosputtering onto heated substrates and varying the  $R$  deposition rate to control the composition. Details of the deposition of these and related compounds has been previously published.<sup>21</sup> Two different compositions were made for each  $R$ :  $R$ : Co nominally 1:5, and 2:17 (except for Ho, where only the 2:17 sample was made). These compositions were chosen because they correspond to the crystalline phases  $(R)\text{Co}_5$  and  $R_2\text{Co}_{17}$ . The composition of each film was verified *ex situ* by energy dispersive x-ray analysis, and was found to vary from the nominal composition in some films as a result of differing rates of re-evaporation for different  $R$ 's. The rare-earth content of each film is given in Table I. Based on these results we separate the films into a Co-rich series (close to 2:17) and a more  $R$ -rich series (close to 1:5 or 1:3). The typical film thickness was 5000 Å, and each sample was subsequently capped with  $\sim 30$  Å of Al to protect the  $R$ -Co film from atmospheric exposure, but still allow the MCD measurements to be performed.

Shown in Fig. 1 is the out-of-plane x-ray diffraction scan from a Pr-Co film that is consistent with  $a$ -axis growth of

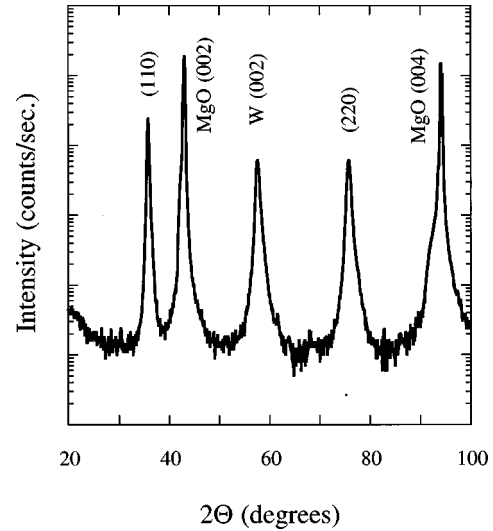


FIG. 1. X-ray-diffraction data from the  $\text{PrCo}_5$  sample, with the  $\text{PrCo}_5$  peaks indexed. The peaks at 43.0 and 94.2 are due to the MgO(100) wafer.

hexagonal  $R$ -Co phases. Similar diffraction scans are observed for all the films studied. Additional x-ray scans and transmission-electron microscopy confirm epitaxial growth with the  $c$  axis in plane, although with two equivalent orientations for  $a$ -axis epitaxy on the fourfold  $W(100)$  buffer layer.<sup>21</sup> From the x-ray-diffraction scans, the  $a$ -axis lattice parameter is determined and given in Table I. From x-ray diffraction (XRD), a determination of the symmetry and lattice parameters of a film is more straightforward than an unambiguous identification of the phase since only one direction of the unit cell is probed in the thin-film scattering geometry. The phase identification is further complicated by the thermodynamic stability of many phases with similar compositions, and, for a given composition, there are often polymorphic forms. Therefore, we identify the known phases that most closely match the measured composition and XRD results.

To determine the magnetic anisotropy fields ( $H_A$ ), the in-plane and out-of-plane hysteresis loops were measured for each film in an extraction magnetometer with a maximum applied field of 9 T. The room temperature out-of-plane measurements for both Pr-Co samples are shown in Fig. 2. These loops along the hard axis show that the anisotropy field is higher in the lower rare-earth content film. This shows the change in anisotropy field that can result from a difference in structure, and points to a role for the Co sublattice in the MCA. All the samples have strong in-plane anisotropy consistent with their  $a$ -axis orientation, but many do not show the in-plane uniaxial anisotropy that might be expected for this structure. This is due to the twinning that results from the two equivalent epitaxial orientations noted above. The anisotropy field is typically on the order of a few Tesla ( $\sim 10$  T for the Sm-Co films).<sup>21</sup> Some of the films also have high room-temperature coercivity, up to 3.1 T. These magnetic measurements are further evidence that the permanent magnet phases of interest are formed in these films.

The magnetic circular dichroism measurements were made using the helical undulator on beamline 5 at the Stanford Synchrotron Radiation Laboratory. This undulator can

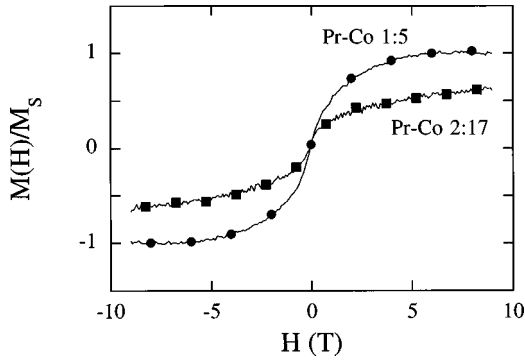


FIG. 2. Magnetization data from the  $\text{PrCo}_5$  and  $\text{Pr}_2\text{Co}_{17}$  samples. This sample has one of the highest anisotropy fields in the entire series,  $<9$  T. The  $\text{SmCo}_5$  sample has  $\sim 10$  T anisotropy field, while most other samples saturated at 3–5 T. Even at the 7 T field used in the MCD experiments, the magnetization perpendicular to the film in the unsaturated samples typically at least 70% of saturation.

produce left-circularly polarized (LCP) or right-circularly polarized (RCP) light on the beam axis.<sup>22</sup> The polarization state is adjusted by shifting the phase between two sets of undulator magnets, and can be set to LCP, RCP, vertical, or horizontal linear, and arbitrary elliptical in between. The degree of polarization for LCP and RCP at the magnetically important  $2p$ - $3d$  core level excitations in the TM's is  $\sim 98\%$ . The undulator light is monochromated, and the incident intensity is monitored by measuring the photocurrent from a Au grid in the path of the monochromatic beam. Samples are placed in a 7 T external field normal to the film plane, with the x-ray beam incident at  $15^\circ$  off normal. Although the film normal is the hard axis, this field is higher than the saturation field except in the case of the Sm-Co samples. It has been shown that in the nonsaturated state, the orbital moment anisotropy causes a noncollinearity of the spin and orbital moments that is observable in the projection of  $\mu_o$  along the measurement axis,<sup>23</sup> and that would require a correction to  $\mu_o/\mu_s$ . However, given that the orbital moment anisotropy is small for these materials, and the samples are nearly saturated ( $H_A \sim 10$  T for Sm-Co), we expect the corrections to be small. All measurements were made with the sample at room temperature. As the incident photon energy is scanned through the Co  $L$  edges, absorption is measured in partial electron yield mode by collecting secondaries with a channeltron detector located along the external field axis about 1 m from the sample. Spin-dependent spectra are obtained by collecting a spectrum at one photon helicity, reversing the helicity, and collecting a second spectrum. Each pair of spectra were typically repeated 2 to 3 times for each sample. A bulk hcp-Co film grown in the same sputtering chamber was also measured for comparison both to the  $R$ -Co compound data and to MCD data from other groups.

### III. RESULTS AND DISCUSSION

All the films show a large dichroism at the Co  $L_{2,3}$  edges, with a typical difference between the left and right circular polarized absorption of  $\sim 40\%$  of the total absorption in the  $L_3$  edge. The spin-dependent absorption spectra, along with their difference, are shown for the more  $R$ -rich Pr-Co sample in Fig. 3. The MCD spectra are summarized for all the

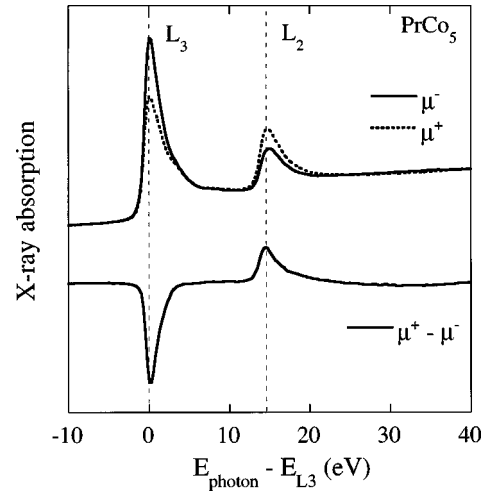


FIG. 3. Polarization dependent x-ray absorption at the Co  $L_{2,3}$  edges measured in partial electron yield mode for  $\text{PrCo}_5$ . The top two curves are the absorption for left and right circular polarized light, and the bottom curve is the difference, or the MCD signal.

samples in Fig. 4. Note the reversal in sign of the MCD signal for the  $R$ -rich Dy-Co sample, which indicates that the applied magnetic field and the Co moment are antiparallel. This reflects the antiferromagnetic coupling of the Co and  $R$  moments in the compounds containing heavy  $R$ s. In all of the other heavy  $R$  samples, this antiferromagnetic coupling is also presumably present, but it is not observed in the sign of the MCD signal because these samples are more Co rich, and the net moment is dominated by the Co moments.

The raw spin-dependent absorption spectra were independently normalized, and if necessary, scaled to match the pre- and post-edge intensities between the two spectra. The difference spectra were then obtained from each of the pairs of normalized spin-dependent spectra, and integrated numerically to obtain values for the integrals in Eq. (1). To obtain the integral over only the  $L_3$  edge, the integration was cut off at the onset of the  $L_2$  edge. Using these numerical integrals, the MCD sum rules were applied to obtain the ratio of the orbital to spin moments ( $\mu_o/\mu_s$ ) and the orbital to net moments ( $\mu_o/\mu_t$ ). The applicability and limitations of the sum rules, in particular for obtaining absolute moments, has been the subject of considerable debate. Most of the controversy has centered on surface effects that can be present in the measurements, and on uncertainties in some of the quantities in Eq. (1), namely,  $n_h$ ,  $\langle T_z \rangle$ , and the background subtraction. We address these uncertainties as they pertain to our measurements below. The quantity  $\mu_o/\mu_s$ , although subject to errors originating in background matching and the choice of integration cutoffs, depends only on the integration of the difference spectrum. Therefore it is not subject to errors originating in the choice of background subtraction or the number of  $3d$ -band holes. Furthermore, although the absolute moments may be subject to errors from overlap of the  $L_3$  and  $L_2$  edges, the difference spectrum is nearly zero by the onset of the  $L_2$  edge and therefore the corresponding error in  $\mu_o/\mu_s$  is small. Another source of error in  $\mu_o/\mu_s$  is the magnetic dipole operator term in the spin sum rule,  $7\langle T_z \rangle/2\langle S_z \rangle$  for which we do not correct. As we will argue below, this correction cannot change the value of  $\mu_o/\mu_s$

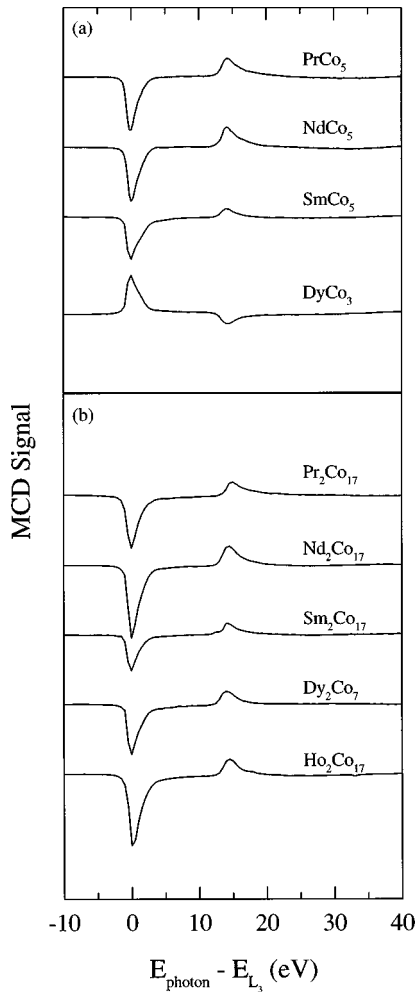


FIG. 4. MCD data ( $I^+ - I^-$ ) for all the Co- $R$  samples. The  $R$ -rich samples are shown in the upper half (a), while the more Co-rich samples are shown in the lower half (b). Note the reversal in sign of the MCD signal for  $\text{DyCo}_3$  which shows that the Co moments are antiparallel to the Dy moments, as expected for the heavy  $R$ 's. In the other heavy  $R$  samples, the Co moments dominate the net moments, so this sign reversal is not seen.

enough to explain all the results. We have also found that  $\mu_o/\mu_t$ , although more dependent on details of the background subtraction and integration cutoffs, shows systematics similar to  $\mu_o/\mu_s$ . This suggests that either  $\mu_o/\mu_s$  or  $\mu_o/\mu_t$  can be used as a normalized indicator of the orbital moments to be compared across samples with different compositions and structures. Based on the dependence of  $\mu_o/\mu_s$  on the various parameters involved in the data analysis, such as the choice of integration cutoffs, we estimate the size of the error bar on  $\mu_o/\mu_s$  for all these measurements at  $\sim 0.05$ .

The hcp-Co film has a  $\mu_o/\mu_s$  value of 0.12. The difference between this measurement and recent transmission MCD measurements taken from polycrystalline Co films (0.095) (Ref. 7) is less than our error bar, and is therefore not significant. Also, the results of band structure calculations of the expected bulk moments show similar values (0.051–0.089).<sup>24,25</sup> An epitaxial bcc-Fe film shows similar correspondence to transmission measurements and calculations. The agreement suggests that in our electron yield measurements, which must be surface sensitive to some degree,

the mean-free path of the collected secondaries is long enough such that the bulk region of the sample is the dominant contribution to the signal. Therefore, assuming that the electron escape depths in the compounds films are similar, and that the films are magnetically homogeneous, surface effects should not be an important contribution to the orbital moments in these measurements. With one exception, all the  $R$ -Co films have enhanced Co orbital moments. In the 2:17 samples,  $\mu_o/\mu_s$  is typically  $\sim 0.25$ , with variations of only  $\sim 0.05$  between different  $R$ 's. The 1:5 samples have higher moment ratios of  $\sim 0.25$ – $0.40$ , with much higher dependence on the  $R$  species. The exception noted above is Pr-Co 1:5, which has a Co orbital moment within the experimental error of that of the hcp-Co film. The values of  $\mu_o/\mu_s$  are summarized, along with composition and structural information for each film in Table I. Note that within the experimental error, the orbital moments of the 2:17 samples are all nearly the same, while the 1:5 samples appear to have a nonmonotonic dependence on the  $4f$ -shell filling.

Before we discuss these trends in the orbital moments, some of the uncertainties arising from the use of the sum rules should be addressed. One additional contribution to the integrals in the spin sum rule is the magnetic dipole term,  $\langle T_z \rangle$ . This term has the effect of increasing the actual spin moment, and thus reducing the moment ratio. In the elemental  $3d$  ferromagnets, the centrosymmetric nature of the structure causes this correction to be small, of order 3%.<sup>17,24,26</sup> However, in noncentrosymmetric systems, this term can be important. The nearest neighbors at some of the Co sites in  $R$ -Co compounds do present such a noncentrosymmetric local environment, so this term must be considered in the present analysis before we can attempt to explain the systematics that are observed. Unfortunately, the size of the dipole term in these particular structures has not been calculated, so estimates based on other calculations must be made. Recent calculations made at TM surfaces suggest that if the dipole term is as large in compounds as at such a surface, a  $\sim 15\%$  correction in the spin moment would be required.<sup>24</sup> This would reduce all the moment ratios, but cannot account for the doubling of the ratio seen in the 2:17 samples or the more than tripling in some of the 1:5 samples. Furthermore, even if the dipole term is large enough to account for all of the enhancement in  $\mu_o/\mu_s$ , the resulting *total* moments would then be unphysically large, or would require a very small number of  $3d$  holes. For this reason, we conclude that the orbital moment enhancement is real, although the magnetic dipole term probably requires a correction to the values reported here. The large orbital moments seen in these measurements therefore point to a possible origin for the large TM sublattice anisotropies in these and related compounds. It is important to note, however, that due to the corrections that may be required for the dipole term and any possible surface effects, the orbital moments observed here cannot be taken as the bulk values for these compounds. Furthermore, MCD does not resolve the distinct Co atomic sites, so any moments derived from the data represent averages over all the Co sites which may be present in a given compound. Therefore, with these limitations in mind, we only compare the orbital-to-spin moment ratios between samples and comment on the trends that occur with structure or composition.

The origin of the orbital moment is surely related to the

local Co structural and electronic environment. All the compounds considered here have expanded Co volumes in relation to bulk hcp Co, which suggests that the 3d bands may be more atomiclike and therefore have less orbital quenching. The larger orbital moments and their variations with  $R$  species in samples with similar composition suggests that the orbital moments are also influenced by the  $R$ . This suggests the possibility of a correlation with the  $R$  4f orbital moment, however we see no such correlation, since all the  $R$ 's in this study have  $L=5$  or 6, assuming trivalent  $R$  ions. The  $\mu_o/\mu_s$  values do appear to correlate roughly with the average Co- $R$  bond lengths, while they do not show any dependence on the average Co-Co bond length (aside from the enhancement in going from bulk hcp Co to the compounds), based on published structural data for each of the phases. In general, the 1:5 samples have longer Co- $R$  bonds than the 2:17 samples, and they also have higher orbital moments.

Aside from these general trends, there are differences in the dependence of orbital moment with 4f shell filling that we now discuss. In general, the Co- $R$  bond lengths are reduced as the 4f shell is filled, due to the lanthanide contraction. It might be expected, then, that the Co 3d bands would broaden and the orbital moments would decrease with 4f filling. In the 2:17 samples, the absence of such a trend is possibly due to the small number of  $R$  nearest neighbors at each Co atom. For bulk  $(R)\text{Co}_5$  compounds, the lattice parameters do not strictly follow the monotonic lanthanide contraction behavior, in particular  $\text{PrCo}_5$  and  $\text{NdCo}_5$  have lattice parameters that are reduced from their expected values based on an interpolation of the lanthanide contraction from the heavy rare earths. The correlation with lattice parameter is still not good, since  $\text{NdCo}_5$  has the largest lattice parameter, but  $\text{SmCo}_5$  has the largest orbital moment. Also, the  $\text{PrCo}_5$  lattice is more expanded than that of  $\text{HoCo}_5$ , but its orbital moment is quenched to the value of hcp-Co metal. These results indicate that the interactions that drive the development of orbital moments in these compounds are more subtle than simple atomic volume arguments alone would suggest, and that effects other than the structural changes are also important.

We therefore must consider the electronic structure of  $R$ -TM compounds for possible mechanisms for the  $R$  species dependence of the orbital moments. The Co 3d bands are subject to hybridization with the  $R$  5d bands, and, if the 4f shells are not completely localized, with the 4f shells as well. These two orbitals behave differently with  $f$ -shell filling, and we discuss them separately below.

The magnetic coupling of the TM to the  $R$  is via an anti-ferromagnetic 3d-5d hybridization interaction.<sup>27,28</sup> As the Co- $R$  bond length is reduced, either by the lanthanide contraction or by a structural transition, the 3d-5d wave function overlap is increased, and Co 3d bands broaden, which reduces the orbital moment. In addition, as one moves along the lanthanide series, 5d bands respond to the increased screening from the 4f shell by shifting up and broadening. These effects, which result in opposing effects on the band overlap, could influence the Co orbital moments. However, the band structures themselves are unknown, as is the effect on the orbital moments.

The 4f shell localization is also dependent on the shell filling. The 4f shell in the lanthanides is well described by

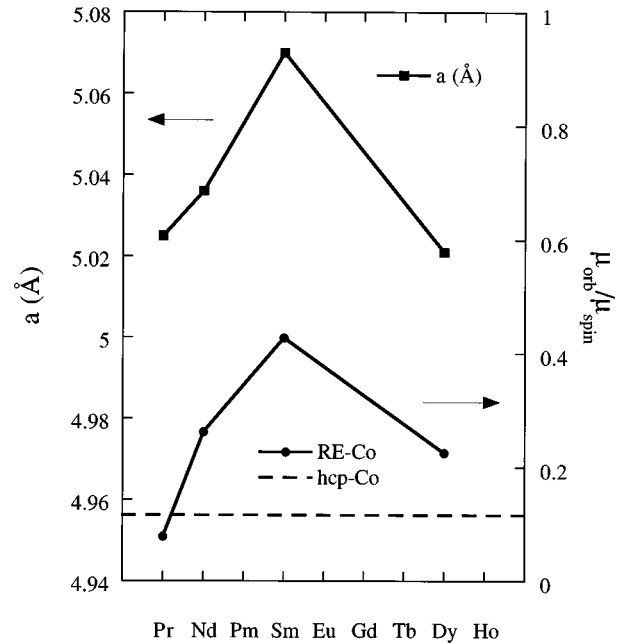


FIG. 5. Orbital to spin moment ratios (lower) and  $a$  lattice parameters (upper) summarized for the  $(R)\text{Co}_5$  samples. Empty squares are x-ray data from the sputtered films, filled squares are published bulk data for  $(R)\text{Co}_5$ , and the dotted line is a fit to the lanthanide contraction. The dashed line shows  $\mu_o/\mu_s$  for the hcp-Co film. This shows that the orbital moments are enhanced, but there is a quenching effect which occurs at the onset of the Ce anomaly in the lattice parameter.

an atomic model, with the exception of Ce compounds, in which it can have significant band character. It is this band-structure effect that drives the well-known anomaly in the lattice parameter at Ce in  $(R)\text{Co}_5$ . As noted above, however, even for Pr and Nd the bulk lattice parameters are reduced from the expected lanthanide contraction behavior, based on an interpolation from La to the heavy  $R$ 's. This behavior is also observed in our lattice parameter data from the 1:5 films, and is shown in Fig. 5 along with the orbital moment data. Note that the orbital quenching is correlated with the onset of the lattice parameter anomaly. This suggests that in Pr and Nd, the 4f electrons still participate in the bonding enough to collapse the lattice parameter, and may also participate in 3d-4f hybridization. With 3d-4f hybridization present in the light  $R$ 's, the Co 3d bands would be significantly affected, and this could change the orbital character of the moments at the Co sites. Above Nd, the 4f shell is presumably well localized and the behavior is dominated by the lanthanide contraction. Although such a delocalization of the 4f shell has been invoked to explain the lattice parameter anomaly in  $\text{CeCo}_5$ ,<sup>29</sup> similar calculations do not exist for the corresponding Pr or Nd compounds. Unfortunately, these calculations do not extend above Ce, and our MCD data do not include the La and Ce compounds, so we cannot make a connection to these calculations with these data. We should also point out that we do not expect to be able to resolve these changes in the Co 3d bands directly in the x-ray absorption spectroscopy data.

While a quantitative treatment of these band-structure effects is not within the scope of this article, we have shown how the deviations from a straightforward magnetovolume

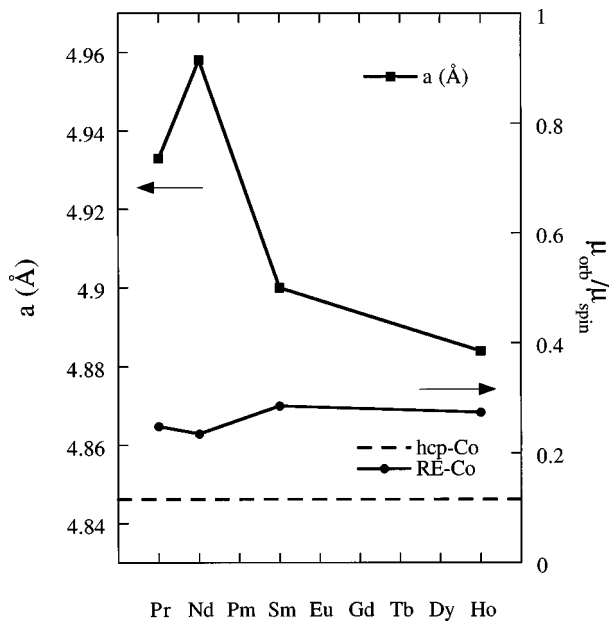


FIG. 6. Same as Fig. 5, but for the lower  $R$  content (2:17) films.

dependence of the Co orbital moments on  $R$   $4f$  shell filling could arise out of details of the  $R$ -TM electronic interactions. For the very light  $R$ 's,  $4f$  shell delocalization results in  $3d$ - $4f$  hybridization, broadening the  $3d$  bands and quenching the orbital moments. For the heavy lanthanides (Sm and heavier), the spatial extent of the  $4f$  shell is reduced by the increased nuclear charge such that the behavior is dominated by the lanthanide contraction, in which the Co  $3d$  bands are broadened primarily via  $3d$ - $3d$  and  $3d$ - $5d$  hybridization as the local volume is reduced. The result is the observed strong quenching of the orbital moment in the Pr and Nd films, with  $\text{SmCo}_5$  possessing the largest Co orbital moment.

We also note that in 2:17 compounds, the Ce lattice parameter anomaly is apparently absent, or is a much smaller effect. This suggests that due to the reduced  $R$  content relative to the 1:5 compounds,  $3d$ - $4f$  hybridization is a smaller effect in these compounds and we can expect less orbital quenching from the light  $R$ 's. In this case the  $R$  dependence of the orbital moment should be determined primarily by the effect of lanthanide contraction on the  $3d$ - $3d$  and  $3d$ - $5d$  hybridization. In Fig. 6 we plot the lattice parameter and orbital moment ratio data for the lower  $R$  content film, on the same vertical scales as in Fig. 5. For these samples we do not see the orbital quenching observed in the Pr- and Nd-Co films. This suggests that any electronic effects observed in the 1:5 case are much smaller effects in the lower rare-earth content samples, which provides further evidence that the development of the orbital moment is driven at least partially by the presence of the  $R$ . We also do not see the lanthanide contraction behavior, but we note that these changes in or-

bitual moment may be more difficult to observe over the experimental errors.

#### IV. SUMMARY

Magnetic circular dichroism measurements were taken at the Co  $L_{2,3}$  edges on a series of epitaxial  $R$ -Co films. The films had nominal composition of either  $R$ :Co 1:5 or 2:17, with  $R$ =Pr, Nd, Sm, Dy, and Ho. Using the MCD sum rules, the orbital to spin moment ratios were extracted from the data. The Co orbital moments in most of the compounds are strongly enhanced as compared to bulk Co, with the 1:5 samples showing the highest orbital moments. The large orbital moment on the TM is presumably the origin of the large TM sublattice contribution to the magnetocrystalline anisotropy energy in many  $R$ -TM permanent magnets. For the 2:17 compounds, the orbital moments do not depend on  $R$  species, while for the 1:5's there is a stronger dependence.

The origin of the orbital moment appears to be related to the local electronic and structural environment at the Co sites. There is a rough dependence on the average Co atomic volume, which arises out of a modulation of the Co  $3d$  bandwidth via the  $3d$ - $3d$  and  $3d$ - $5d$  hybridization interactions. An analysis of Co-Co and Co- $R$  bond distances from bulk structural data suggests that this volume dependence is driven mainly by the Co- $R$  bond distance. In the 1:5 compounds, the Co orbital moments in the Pr and Nd samples are quenched to lower values than is expected from the magnetovolume dependence. This is attributed to a significant  $4f$  band character in the very light  $R$ 's, similar to that which drives the Ce anomalies in  $(R)\text{Co}_5$ , resulting in  $3d$ - $4f$  hybridization. Above Nd, the  $4f$  shell is well localized and the behavior is determined primarily by the lanthanide contraction. The absence of these effects in the 2:17 compounds is interpreted as resulting from the lower  $R$  content, such that both the effects of  $3d$ - $4f$  hybridization and the lanthanide contraction are lost within the error bar on the orbital moment. These results show how subtle changes in crystal and electronic structure can be important in determining the intrinsic magnetic properties of  $R$ -TM compounds. Furthermore, they point out the need for more complete evaluations of the band structure of these isostructural compounds for a more complete understanding of the magnetic interactions in  $R$ -TM intermetallics.

#### ACKNOWLEDGMENTS

We gratefully acknowledge Piero Piannetta of SSRL for the use of the high-field magnet endstation, and Dale Koelling of ANL for helpful discussions. This work is supported by the United States Department of Energy office of Basic Energy Sciences under Contract Nos. W-31-109-ENG-38 (ANL), DE-AC03-76SF00515 (SSRL), and W-7405-ENG-48 (LLNL).

<sup>1</sup>J. F. Herbst, *Rev. Mod. Phys.* **63**, 819 (1991).

<sup>2</sup>K. H. J. Buschow, *Rep. Prog. Phys.* **54**, 1123 (1991).

<sup>3</sup>J. M. Alameda, D. Givord, R. Lemaire, and Q. Lu, *J. Appl. Phys.* **52**, 2079 (1981).

<sup>4</sup>B. Matthaei, J. J. M. Franse, S. Sinnema, and R. J. Radwanski, *J. Phys. (Paris) Colloq.* **49**, C8-553 (1988).

<sup>5</sup>R. Ballou, B. Gorges, R. Lemaire, H. Rakoto, and J. C. Ousset, *Physica B* **155**, 266 (1989).

<sup>6</sup>S. Hirosawa, K. Tokuhara, H. Yamamoto, S. Fujimura, M. Sogawa, and H. Yamauchi, *J. Appl. Phys.* **61**, 3571 (1987).

<sup>7</sup>R. Grössinger, X. K. Sun, H. R. Eibler, K. H. J. Buschow, and H. R. Kirchmayr, *J. Magn. Magn. Mater.* **58**, 55 (1986).

- <sup>8</sup>J. Schweizer and F. Tasset, *J. Phys. F* **10**, 2799 (1980).
- <sup>9</sup>L. Nordström, M. S. S. Brooks, and B. Johansson, *J. Magn. Magn. Mater.* **104-107**, 1942 (1992).
- <sup>10</sup>G. Schütz, W. Wagner, W. Wilhelm, P. Keinle, R. Zeller, R. Frahm, and G. Materlike, *Phys. Rev. Lett.* **58**, 737 (1987).
- <sup>11</sup>J. G. Tobin, G. D. Waddill, A. F. Jankowski, P. A. Sterne, and D. P. Pappas, *Phys. Rev. B* **52**, 6530 (1995).
- <sup>12</sup>J. G. Tobin, G. D. Waddill, and D. P. Pappas, *Phys. Rev. Lett.* **68**, 3642 (1992).
- <sup>13</sup>C. T. Chen, F. Sette, Y. Ma, and S. Modesti, *Phys. Rev. B* **42**, 7262 (1990).
- <sup>14</sup>C. T. Chen, Y. U. Idzerda, H.-J. Lin, G. Meigs, A. Chaiken, G. A. Prinz, and G. H. Ho, *Phys. Rev. B* **48**, 642 (1993).
- <sup>15</sup>B. T. Thole, P. Carra, F. Sette, and G. van der Laan, *Phys. Rev. Lett.* **68**, 1943 (1992).
- <sup>16</sup>P. Carra, B. T. Thole, M. Altarelli, and X. Wang, *Phys. Rev. Lett.* **70**, 694 (1993).
- <sup>17</sup>C. T. Chen, Y. U. Idzerda, H.-J. Lin, N. V. Smith, G. Meigs, E. Chaban, G. H. Ho, E. Pellegrin, and F. Sette, *Phys. Rev. Lett.* **75**, 152 (1995).
- <sup>18</sup>X. Wang, V. P. Antropov, B. N. Harmon, J. C. Lang, and A. I. Goldman, *J. Appl. Phys.* **75**, 6366 (1994).
- <sup>19</sup>P. Fischer, G. Schütz, and G. Wiesinger, *Solid State Commun.* **76**, 777 (1990).
- <sup>20</sup>J. Chaboy, A. Marcelli, L. M. Garcia, J. Bartolome, M. D. Kuz'min, H. Maruyama, K. Kobayashi, H. Kawata, and T. Iwazumi, *J. Magn. Magn. Mater.* **104-107**, 1051 (1995).
- <sup>21</sup>E. E. Fullerton, C. H. Sowers, J. E. Pearson, X. Z. Wu, D. Lederman, and S. D. Bader, *Appl. Phys. Lett.* **69**, 2438 (1996).
- <sup>22</sup>S. Lidia and R. Carr, *Nucl. Instrum. Methods Phys. Res. A* **347**, 77 (1994).
- <sup>23</sup>H. A. Dürr and G. van der Laan, *J. Appl. Phys.* **81**, 5355 (1997).
- <sup>24</sup>R. Wu and A. J. Freeman, *Phys. Rev. Lett.* **73**, 1994 (1994).
- <sup>25</sup>P. Söderlind, O. Eriksson, B. Johansson, R. C. Alberts, and A. M. Boring, *Phys. Rev. B* **45**, 12 911 (1992).
- <sup>26</sup>R. Wu, D. Wang, and A. J. Freeman, *Phys. Rev. Lett.* **71**, 3581 (1993).
- <sup>27</sup>M. S. S. Brooks, L. Nordström, and B. Johansson, *Physica B* **172**, 95 (1991).
- <sup>28</sup>I. A. Campbell, *J. Phys. F* **2**, L47 (1972).
- <sup>29</sup>L. Nordström, O. Eriksson, M. S. S. Brooks, and B. Johansson, *Phys. Rev. B* **41**, 9111 (1990).